


Article

Wheat Seed Phenotype Detection Device and Its Application

Haolei Zhang ¹, Jiangtao Ji ^{1,2}, Hao Ma ^{1,2}, Hao Guo ¹, Nan Liu ¹ and Hongwei Cui ^{1,*} 

¹ College of Agricultural Equipment Engineering, Henan University of Science and Technology, Luoyang 471000, China

² Longmen Laboratory, Luoyang 471000, China

* Correspondence: chw19900405@126.com; Tel.: +86-13664302731

Abstract: To address the problem of low efficiency and automatically sense the phenotypic characteristics of wheat seeds, a wheat seed phenotype detection device was designed to predict thousand seed weight. Five commonly used varieties of wheat seeds were selected for the study, and a wheat seed phenotype detection system was built with a 2 mm sampling hole plate. Grayscale, image segmentation, area filtering and other methods were used to process the image in order to extract and analyse the correlation between thousand seed weight and seven phenotypic characteristics: wheat seed area, perimeter, long axis, short axis, ellipticity, rectangularity, and elongation. The results showed that different varieties of wheat seeds were significantly correlated with different phenotypic characteristics. Among them, the area and short axis for Luomai 26; the area, long axis, short axis, perimeter, and rectangularity for Jinqiang 11; the area and perimeter for Zhoumai 22; the area of Luomai 42; the area, short axis, and perimeter for Bainong 207 were significantly correlated with the thousand seed weight. A multiple linear regression model of thousand seed weight prediction was developed by selecting the significantly correlated phenotypic characteristic. The models showed that the R^2 values of the thousand seed weight prediction models for Jinqiang 11 and Bainong 207 were 0.853 and 0.757, respectively; and the R^2 values for Luomai 26, Zhoumai 22, and Luomai 42 were less than 0.5. Subsequently, PCA-MLR was used to build a thousand seed weight prediction model, and K-fold cross-validation was used for comparative analysis. Afterwards, three kinds of wheat seeds with 40–50 g thousand seed weight were selected to validate the model. The validation results showed that the more significantly correlated the phenotypic parameters were, the higher the accuracy of the thousand seed weight prediction model. The study provided a set of detection devices and methods for the rapid acquisition of the phenotypic characteristics of wheat seeds and thousand seed weight prediction.

Keywords: wheat seed; detection devices; phenotypic characteristics; thousand seed weight



Citation: Zhang, H.; Ji, J.; Ma, H.; Guo, H.; Liu, N.; Cui, H. Wheat Seed Phenotype Detection Device and Its Application. *Agriculture* **2023**, *13*, 706. <https://doi.org/10.3390/agriculture13030706>

Academic Editors: Arthur Novikov, Clíssia Barboza Mastrangelo and Paweł Tylek

Received: 14 February 2023

Revised: 14 March 2023

Accepted: 15 March 2023

Published: 18 March 2023



Copyright: © 2023 by the authors. Licensee MDPI, Basel, Switzerland. This article is an open access article distributed under the terms and conditions of the Creative Commons Attribution (CC BY) license (<https://creativecommons.org/licenses/by/4.0/>).

1. Introduction

Wheat is a major grain crop in China, with a planting area of approximately 230 million hm^2 and an annual production of approximately 1.3 billion t [1]. The selection of good varieties of wheat seeds is a prerequisite for ensuring wheat yield, and it contributes to wheat quality; wheat seed phenotypic characterization is a key to determining if wheat seeds are high-quality [2]. Determining the quality of wheat seeds involves characteristic parameters, including the size and fullness characteristics of the seeds. The sizes of same-variety wheat seeds directly affect the germination rate and thus the wheat yield; wheat seed fullness is an important factor in determining wheat yield and quality, and it serves as a comprehensive evaluation index of the ecological suitability of wheat [3]. Therefore, the accurate detection of the phenotypic characteristic parameters of wheat seeds is important for selecting and farming new varieties of wheat seeds, and it helps to improve the wheat quality and ensure food security [4].

Traditional extraction of phenotypic information from wheat seeds is performed manually; this method is inefficient, laborious, and prone to large errors, randomness, and

poor precision in measurements by different personnel; thus, the traditional method of phenotypic information extraction is considered a major bottleneck affecting the selection and breeding of new varieties [5–9]. Image processing techniques have the advantages of being fast and nondestructive; with significant improvements in image processing techniques, they are widely used in agricultural production activities, and high-throughput seed phenotype detection has become an emerging technology in precision agriculture that has received the attention of many researchers [10,11]. Korohou T. et al. [12] proposed a method for estimating wheat seed yield based on a combination of the morphological characteristics of organs and the quality of wheat. Zhang et al. [13] designed an image analysis system to determine the morphological characteristics of wheat seed appearance and used computer image processing and analysis techniques to determine various morphological parameters, such as the long axis, short axis, and projected area characteristics of wheat seeds. Li et al. [14] designed a machine vision-based vegetable seed vigour index detection system, and the results showed that the system was more than 92% accurate relative to the seed vigour index calculated by manual measurement. Zhao et al. [4] studied a high-throughput phenotyping system for wheat seeds based on image analysis. The system was implemented to analyse the colour and morphology characteristics of wheat seeds, and the researchers designed an operator interface to display the measurement results. S. Ma Jumdar et al. [15] combined three features—wheat, barley, rye, and oats—in pairs, and the researchers studied the morphology, colour, and texture; the results showed that the best results were obtained by combining the features for classification identification. Wang et al. [16] used a watershed algorithm to segment wheat images, extracted morphological and colour feature parameters, and combined the information with an artificial neural network back propagation (BP) algorithm to establish a wheat appearance quality evaluation model; the average recognition rate reached 93%. Although the above studies have good detection and overall classification results for images of seeds [17] and the classification of individual seeds in images [18,19], the application of image analysis techniques in wheat seed detection is not perfect; the relationships between the phenotypic parameters and thousand seed weight of wheat seeds have not been studied globally, thereby failing to provide a strong basis for applying image processing techniques in wheat seed selection and breeding processes. In this paper, we establish a wheat seed phenotype detection system based on image analysis techniques [20–23] combined with machine learning [24–27], and we conduct research on wheat seed phenotype characteristic detection methods and thousand seed weight prediction models to provide a reference for wheat seed phenotype detection systems.

In this paper, we established a wheat seed phenotype detection system, analysed the correlations between phenotypic characteristic parameters and thousand seed weight, and established a thousand seed weight prediction model. The main objectives include the following: (1) To establish a wheat seed phenotype characteristic detection system; (2) To use image processing and other techniques to extract phenotype characteristic parameters, such as wheat seed area, perimeter, long axis, short axis, ellipticity, rectangularity, and elongation; (3) To analyse the correlations between the characteristic parameters and wheat seed thousand seed weight, and to establish and validate a wheat seed thousand seed weight prediction model.

2. Data and Methods

2.1. Wheat Seed

Wheat seeds with widely phenotypic and morphological characteristic differences were collected from local common species in Luoyang, Henan Province: Jinqiang 11, Luomai 26, Luomai 42, Zhoumai 22, and Bainong 207. Among these regions, Jinqiang 11 has red seeds, and its thousand seed weight is 44.3 g; Luomai 26 has white seeds, and its thousand seed weight is 44.9 g; Luomai 42 has red seeds, and its thousand seed weight is 50.7 g; Zhoumai 22 has white seeds, and its thousand seed weight is 45.4 g; and Bainong 207 has white seeds, and its thousand seed weight is 41.7 g.

2.2. Wheat Seed Phenotypic Characteristic Detection System

2.2.1. Image Acquisition Device

A wheat seed image acquisition device was designed, as shown in Figure 1, including a camera (SY8031, Shenzhen Weixin Vision Technology Company, Shenzhen, China), a dark box (self-design), four light-emitting diode (RGB LEDs) strip light sources (T5F06, Rays Lighting, Huizhou, China), a sampling hole plate (128.5 × 83 mm, 10 × 10 holes, self-design), and a computer.

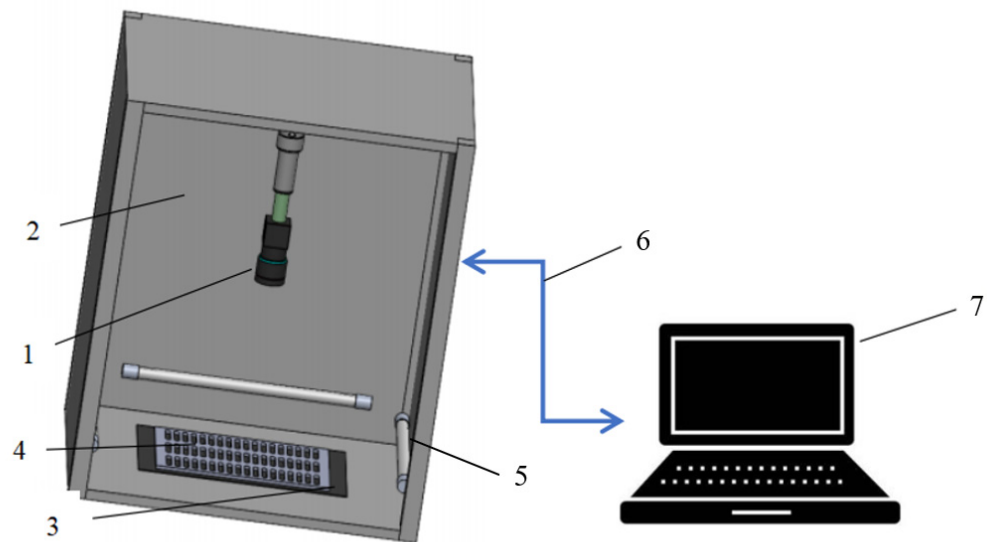


Figure 1. Wheat seed image acquisition device. 1. USB camera. 2. Dark box. 3. Light-absorbing fabric. 4. Sampling hole plate. 5. strip light sources. 6. Cable. 7. Computer.

2.2.2. Sampling Hole Plate

Fifty seeds from the five experimental varieties of wheat were measured. The average long axes and short axes of wheat seeds are 6–7 mm and 3–4 mm, respectively. Therefore, the holes were designed to be 9 × 5 mm, the hole depths were 3, 2, and 1 mm. The plate size was designed to be 128.5 × 83 mm, and the number of holes in the plate was 100. The wheat seed phenotype detection device was used to measure each type of wheat seed 20 times on three kinds of sampling hole plates to obtain the mean value of wheat seed phenotype characteristic parameters, and manually measure the long axis and short axis of the same batch of seeds. The error of the wheat seed phenotype detection device in detecting the long axis and the short axis and the variance of each parameter was analysed, as shown in Tables 1 and 2. The appropriate sampling hole plate was selected according to the errors and variances.

Table 1. Average errors of different hole plates for detecting long and short axes.

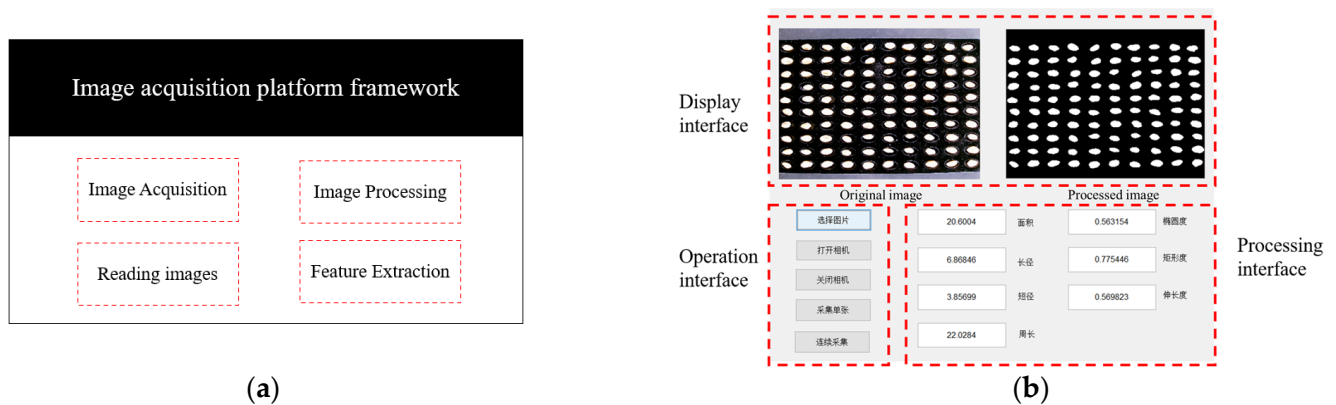
Varieties	Average Errors of 1 mm Hole Plate (mm)	Average Errors of 2 mm Hole Plate (mm)	Average Errors of 3 mm Hole Plate (mm)
Luomai 26	0.199362	0.296986	0.492199
Jinqiang 11	0.093554	0.199852	0.631647
Zhoumai 22	0.148807	0.216848	0.422150
Luomai 42	0.146492	0.289650	0.316111
Bainong 207	0.341720	0.081696	0.402236

Table 2. Variances in different hole plate detection characteristic parameters.

Hole Plate	Varieties	Variance							Total Variance
		Area	Long Axis	Short Axis	Perimeter	Ellipticity	Rectangularity	Elongation	
1 mm	Luomai 26	0.0422	0.0024	0.0009	0.0337	0.0000	0.0000	0.0009	0.0802
	Jinqiang 11	0.0151	0.0012	0.0003	0.0100	0.0000	0.0002	0.0000	0.0269
	Zhoumai 22	0.0151	0.0042	0.0008	0.0133	0.0000	0.0000	0.0000	0.0334
	Luomai 42	0.0241	0.0060	0.0015	0.0181	0.0000	0.0000	0.0000	0.0497
	Bainong 207	0.0404	0.0015	0.0008	0.0258	0.0000	0.0000	0.0001	0.0686
2 mm	Luomai 26	0.0006	0.0000	0.0000	0.0002	0.0000	0.0000	0.0003	0.0011
	Jinqiang 11	0.0031	0.0001	0.0001	0.0007	0.0000	0.0000	0.0000	0.0040
	Zhoumai 22	0.0002	0.0000	0.0000	0.0001	0.0000	0.0000	0.0000	0.0004
	Luomai 42	0.0026	0.0001	0.0000	0.0008	0.0000	0.0000	0.0010	0.0044
	Bainong 207	0.0521	0.0002	0.0001	0.0001	0.0000	0.0000	0.0007	0.0533
3 mm	Luomai 26	0.0087	0.0006	0.0002	0.0068	0.0000	0.0000	0.0022	0.0185
	Jinqiang 11	0.0745	0.0033	0.0011	0.0404	0.0000	0.0000	0.0023	0.1217
	Zhoumai 22	0.0067	0.4495	0.0001	0.0016	0.0000	0.0000	0.0010	0.4588
	Luomai 42	0.0291	0.0019	0.0008	0.0217	0.0000	0.0000	0.0000	0.0534
	Bainong 207	0.0076	0.0004	0.0001	0.0283	0.0000	0.0000	0.0000	0.0365

2.2.3. Image Acquisition Software Platform

The image acquisition software platform was developed using MATLAB GUI (MATLAB 2020b, MathWorks, Natick, MA, USA); the system architecture consists of four parts: image acquisition, image processing, image reading, and feature extraction. The software platform architecture and system interface are shown in Figure 2. The image can be collected individually and continuously, and it is automatically stored in the hard disk after the acquisition is complete. The image is read either from the real-time acquired image or the stored image. After the image is read into the system, the software platform uses image preprocessing, image segmentation, feature extraction, and other steps to obtain wheat seed phenotype characteristic parameters.

**Figure 2.** Software platform architecture (a) and interface (b).

2.2.4. Wheat Seed Phenotyping Detection Process

The flow chart of wheat seed image processing is shown in Figure 3. After the image is read into the software, the image is greyed out and binarized. Then, the noise is filtered using the area filtering method. After that, the holes are filled by the morphological operations. Finally, the phenotypic characteristic parameters of wheat seeds are extracted from the processed image.

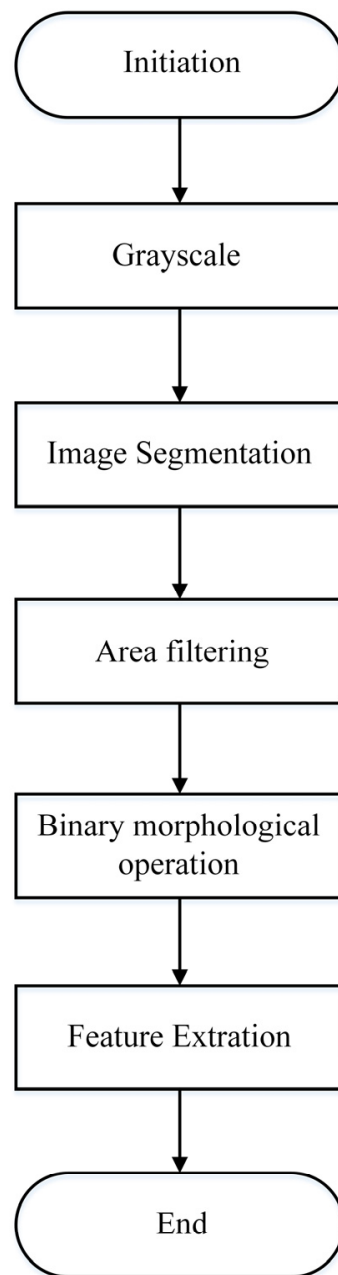


Figure 3. Image processing and analysis block diagram.

2.3. Image Acquisition Methods

Before image acquisition, the camera was mounted. Camera mounting height was approximately 97 mm to make the sampling hole plate appear completely in the camera field of view. The camera field of view was 124×93 mm, the sampling hole plate appeared completely in the field of view, and the image resolution was 3264×2448 pixels. After the camera was installed, the wheat seeds were laid on the sampling plate to ensure that there was one wheat seed in each sampling hole, and the lights were turned on. Then, the sampling plate was placed vertically below the camera to ensure that the sampling plate was in the camera field of view. After that, the images (32-bit) were acquired, and phenotypic parameters of wheat seeds were extracted. The camera installation and sampling plate arrangement are shown in Figure 4.

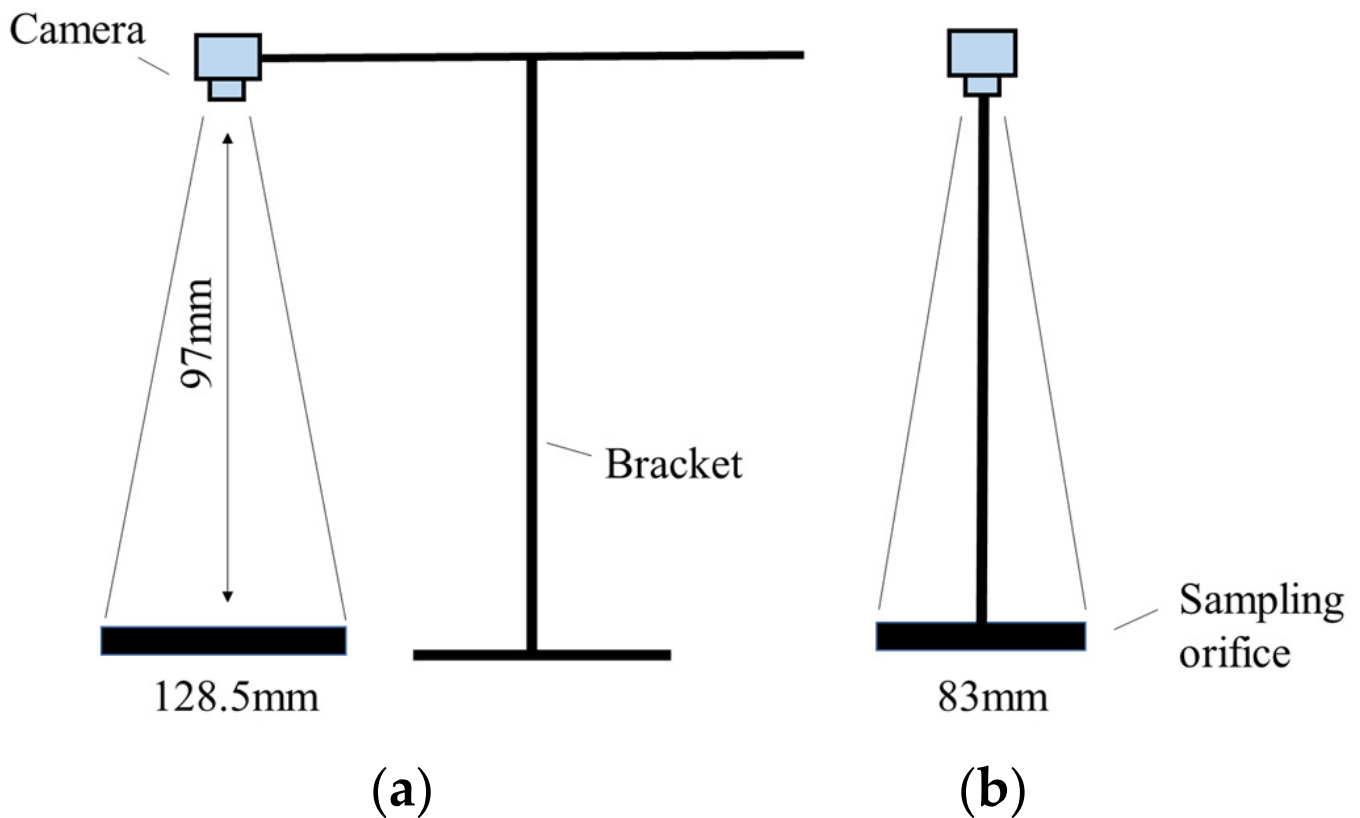


Figure 4. Diagram of camera installation. The plate size was designed to be 128.5 × 83 mm. The camera field of view was 124 × 93 mm, and the image resolution was 3264 × 2448 pixels. (a) Left view. (b) Front view.

2.4. Image Preprocessing

There is noise in the image due to background, sample plate reflection, and other reasons, so image meet to be preprocessed. First, four methods are compared to greyscale images using the contrast component, maximum, average, and weighted average methods. According to the differentiation of wheat seeds from the background in Figure 5b, the maximum method was selected to greyscale the images. Then, the binarization effects of the greyscale histogram-based threshold selection, the Otsu method, and the iterative method [28] are compared. According to the difference in the separation of wheat seed edges from the background in Figure 5c, the Otsu algorithm is selected to binarise the images. However, there is still noise in Figure 5c. To eliminate those noise, the area filtering method is selected to filter the image noise. The pixel area filtering range is determined by repeating the test several times for pixels less than 800 and greater than 20,000; the results are shown in Figure 5d. Figure 5d shows that holes exist in the middle part of the seeds. To fill the holes, the images are processed by applying hole filling (Figure 5e), open operation (Figure 5f), and closed operation (Figure 5g) [29] to eliminate the holes inside the seeds and smooth the seed boundaries.

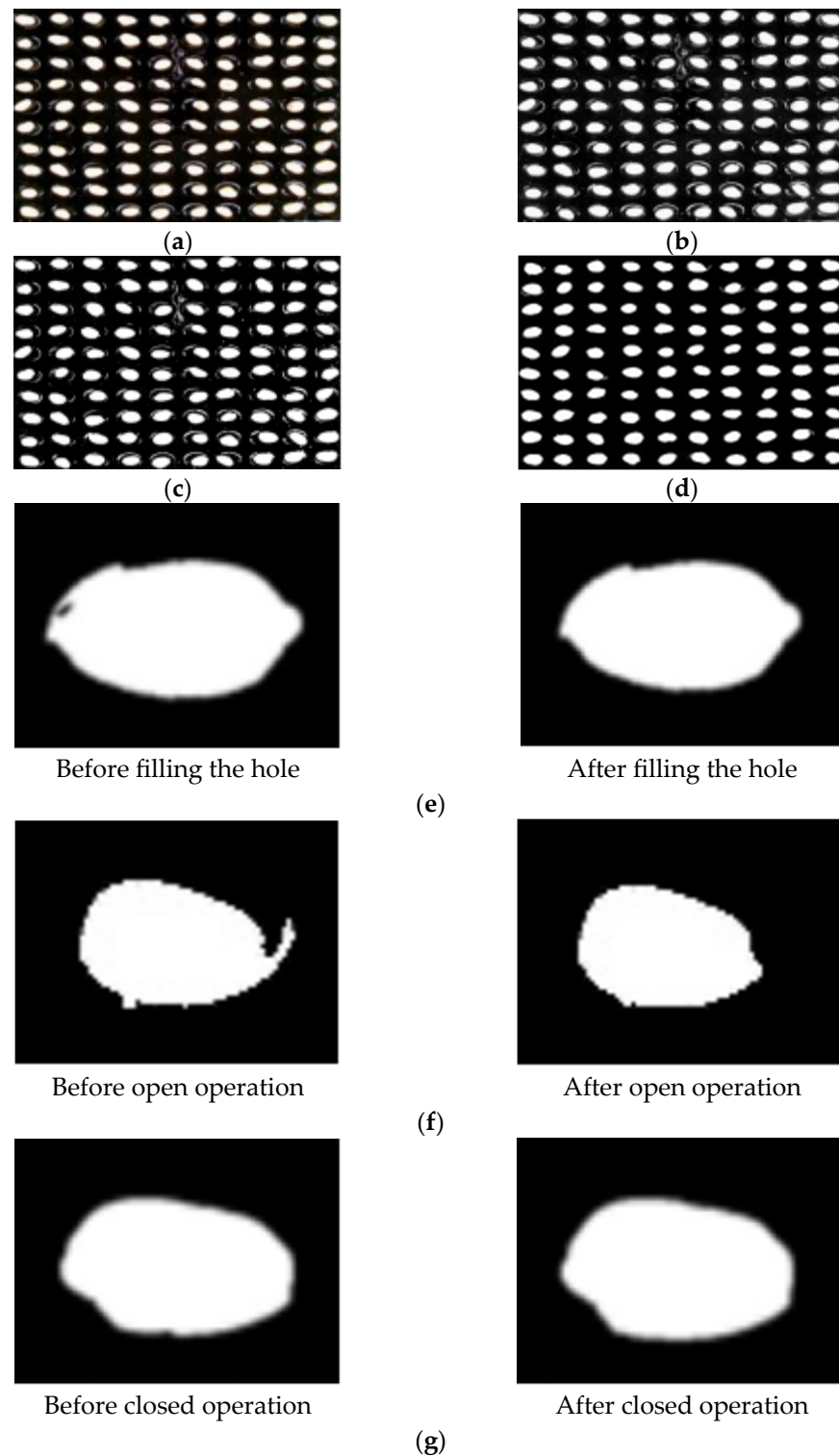


Figure 5. Wheat seed image preprocessing results. Select the maximum method to grayscale the image, and then adopt the Otsu algorithm to binary the image. Choose the area filtering algorithm to filter the image noise. The basic binary morphological operations used in this paper to apply hole filling and two complex morphological operators—open operation and closed operation, which effectively eliminate the holes in the wheat seeds, and smooth the boundary of the wheat seeds. (a) Original image. (b) Greyscale image. (c) Binarized image. (d) Area filtered image. (e) Comparison chart of hole filling. (f) Comparison image of open operation. (g) Comparison image of closed operation.

2.5. Feature Extraction

The results of Gegas et al. [30] show that the area, long axis, short axis, and ratio of long axis to short axis characteristics of wheat seeds are related to the thousand seed weight of wheat seeds. Therefore, we extract seven phenotypic characteristics of wheat seeds—area, long axis, short axis, perimeter, ellipticity, rectangularity, and elongation—and study correlations between the seven phenotypic characteristics and the thousand seed weight. The wheat seed area is pixel area A of the connected area (Equation (1)).

$$A = \sum_{x,y \in R} f(x,y) \quad (1)$$

where the image $f(x,y)$ consists of multiple pixel points, and x and y denote the X -axis and Y -axis coordinates of the pixel points, respectively.

The long axis length a is the maximum distance between two points of the seed edge, and the short axis length b is distance of intersection points determined by the perpendicular bisector of the long axis and points of the wheat seed edge. The slope of long axis is Equation (3). When $K \neq 0$, the points where the wheat seed pixel is 0 are substituted into Equation (4); if the equation is satisfied, 0 pixel points represent the end points of the short axis, and the short axis length is obtained by using Equation (5). If $K = 0$, the transverse coordinate of the endpoint of the short axis has the same value as the transverse coordinate of the midpoint of the long axis. The coordinates of the seed edge points are obtained with the same value of the transverse coordinate, and Equation (5) is used to calculate the short axis length.

$$a = \sqrt{(x_2 - x_1)^2 + (y_2 - y_1)^2} \quad (2)$$

$$K = \frac{y_2 - y_1}{x_2 - x_1} \quad (3)$$

$$y = -\frac{1}{K}(x - x_m) + y_m \quad K \neq 0 \quad (4)$$

$$b = \sqrt{(x_{m2} - x_{m1})^2 + (y_{m2} - y_{m1})^2} \quad (5)$$

where the coordinates of the leftmost and rightmost pixel points of the wheat seed are (x_1, y_1) and (x_2, y_2) , respectively. Their midpoint coordinates are (x_m, y_m) , the slope of long axis is K , and the endpoint coordinates are (x_{m1}, y_{m1}) and (x_{m2}, y_{m2}) , respectively.

The perimeter L is the boundary length of the target seed in the image, and the contour points are extracted in a clockwise or counterclockwise manner. Then, the relationship between the contour point and the next contour point is evaluated. The number of pixels is recorded as N_a if the relationship is labelled 4 connectivity relationship. If the relationship is labelled 8 connectivity relationship, the number of pixels is recorded as N_b . The ellipticity O indicates the degree to which the seed tends to be elliptical (Equation (7)). The rectangularity R [31] indicates the degree to which the wheat seed fills its smallest external rectangle (Equation (8)). Elongation E indicates the degree of slenderness of the wheat seed (Equation (9)).

$$L = N_a + \sqrt{2}N_d \quad (6)$$

$$O = \frac{b}{a} \quad (7)$$

$$R = \frac{A}{a \times b} \quad (8)$$

$$E = \frac{\min(a,b)}{\max(a,b)} \quad (9)$$

Since the parameters obtained by the above method are in the pixel space, they must be converted to the world space. In this paper, the image resolution is 3264×2448 pixels,

and the actual image space size is 124×93 mm. Thus, the actual size of image element is 0.3799×0.376 mm.

2.6. Thousand Seed Weight Measurement Method

The thousand seed weight is an important parameter to measure the quality of wheat seeds, and it is also an important indicator of the size and fullness characteristics of wheat seeds. The higher the thousand seed weight is, the higher the maturity and fullness characteristics of wheat seeds, and the smaller the proportion of broken grains. In this paper, the 100-seeds method is used to measure the thousand seed weight, as shown in Figure 6. 100 seeds are randomly selected from pure wheat seeds mixed well and weighed on an electronic scale. This is repeated three times to take the average value as 100 wheat seed masses and converted to obtain the thousand seed weight. Each kind of wheat seed is subjected to the above steps to detect its thousand seed weight.



Figure 6. Thousand seed weight measurement by the 100-seeds method. 1. Wheat seed. 2. Display interface. 3. Counting unit. 4. Scaling unit.

2.7. Model Construction and Accuracy Evaluation

The seven phenotypic parameters were used as independent variables and wheat thousand seed weight was used as dependent variable to establish wheat thousand seed weight prediction models based on multiple linear regression. Correlation coefficients and principal component analysis were used to determine the input variables of the models to analyse the stability of different models in K-fold cross-validation. The coefficient of determination (R^2) and root mean square error ($RMSE$) were used to evaluate the accuracy of the wheat thousand seed weight prediction model. The closer R^2 was to 1, the lower the $RMSE$, and the higher the accuracy of the prediction model. The formula is as follows:

$$R^2 = \frac{\sum_{i=1}^n (x_i - \bar{x})^2 \times (y_i - \bar{y})^2}{\sum_{i=1}^n (x_i - \bar{x})^2 \times \sum_{i=1}^n (y_i - \bar{y})^2} \quad (10)$$

$$RMSE = \sqrt{\frac{\sum_{i=1}^n (y_i - x_i)^2}{n}} \quad (11)$$

where x_1, \bar{x} are the measured thousand seed weight and average thousand seed weight, respectively, while y_1, \bar{y} are the predicted thousand seed weight and average thousand seed weight, respectively; n is the number of samples.

3. Results and Discussion

3.1. Effect of Sampling Hole Plate on Parameters

To select the sampling hole plate, 100 wheat seed samples were measured by the system each time. Then, 10 wheat seeds were randomly connected in an end-to-end manner, and their long and short axis lengths were measured as the standard long and short axes lengths using a Vernier calliper to calculate the average error of the system, as shown in Table 1. Twenty measurements were made on three plates for each type of wheat seed, and the variance in the system was analysed to measure the phenotypic characteristic parameters, as shown in Table 2.

3.1.1. Average Error

The average error of the software in detecting the long and short axis of wheat seeds is shown in Table 1.

As shown in Table 1, for Luomai 26, Jinqiang 11, Zhoumai 22, and Luomai 42, the average error of the 1 mm hole plate detection is the smallest; for Bainong 207, the average error of the 2 mm hole plate detection is the smallest. The errors of the 2 mm hole plate detection are not much different from those of the 1 mm hole plate detection, which are 0.1 mm, 0.1 mm, 0.07 mm, 0.14 mm, and -0.26 mm, respectively. Thus, it can be seen that both the 1 mm and 2 mm plates can detect the phenotypic characteristics of wheat seeds.

3.1.2. Variance

The variances in the phenotypic characteristic parameters of different kinds of wheat obtained on different plates are shown in Table 2. The smaller the variance is, the lower the dispersion of the detected characteristic parameters, and the fewer the number of errors in the detected characteristic parameters of the software.

According to Table 2, from the five species (except for Bainong 207), the smallest parameter variance was detected by using the 2 mm hole plate for image acquisition. To detect the least errors and fluctuation of characteristic parameters, the 2 mm sampling hole plate is selected as the best hole plate.

3.2. Distribution of Phenotypic Characteristic Parameters of Wheat Seeds

One hundred seeds of varieties are randomly selected and tested for seven phenotypic characteristics—area, long axis, short axis, perimeter, ellipticity, rectangularity, and elongation—using the wheat seed phenotypic characteristic detection system. A box line diagram of each characteristic parameter is shown in Figure 7.

For Luomai 26, Figure 7f shows that the highest median line of Luomai 26 means the largest rectangularity, which indicates that the seeds filling the smallest outer minimum rectangle are the most numerous.

For Jinqiang 11, as shown in Figure 7b, the highest median line position of Jinqiang 11 indicates a longer perimeter. Figure 7c shows that the median line position of Jinqiang 11 is the highest, indicating that its long axis is longer, which shows that the long axis determines the size of the perimeter to a certain extent. As shown in Figure 7d, the lowest box position of Jinqiang 11 indicates that this seed has the smallest short axis. Jinqiang 11 had the lowest box position, indicating the smallest ellipticity level in Figure 7e. In Figure 7g, the lowest median line of Jinqiang 11 indicates the smallest average level of elongation length and a higher seed slenderness, which are consistent with the narrowed appearance of seeds.

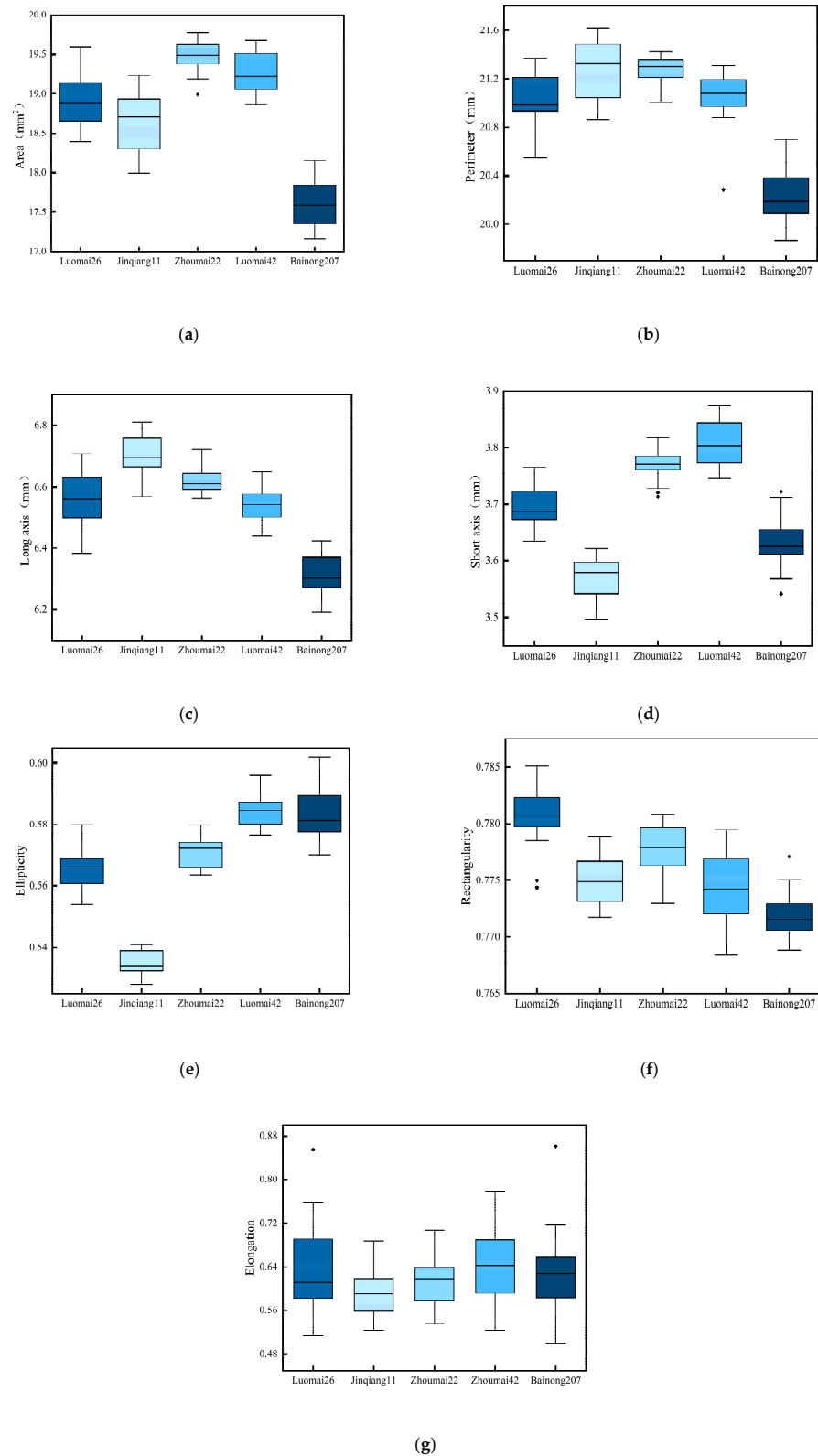


Figure 7. Distribution of seven phenotypic characteristic parameters of wheat seeds. The middle line of box is the median of the characteristic parameters and represents the average level of the characteristic parameters. The upper and lower limits of box are the upper quartile and the lower quartile of the characteristic parameters. Above and below the box, two lines represent the maximum and minimum values, respectively. (a) Area. (b) Perimeter. (c) Long axis. (d) Short axis. (e) Ellipticity. (f) Rectangularity. (g) Elongation.

For Zhoumai 22, the box position of Zhoumai 22 is higher, the median line position is the highest and the box volume is the smallest, indicating that the seed area of Zhoumai 22 is the largest and the measurement results fluctuate less in Figure 7a.

For Luomai 42, the highest box position of Luomai 42 indicates that this seed has the longest short axis (wider seeds) in Figure 7d. The median line position of Luomai 42 is the highest, indicating that the ellipticity level of Luomai 42 is the largest in Figure 7e. The highest median line of Luomai 42 indicates the largest average level of elongation length and a lower seed slenderness in Figure 7f.

For Bainong 207, the box and median line position of Bainong 207 are the lowest, indicating that this seed area is the smallest and mostly distributed below 18 mm² in Figure 7a. As shown in Figure 7b, the lowest median line position of Bainong 207 indicates a smallest perimeter. Figure 7c shows that the median line position of Bainong is the lowest, indicating that its long axis is shortest, which shows that the long axis and short axis determine the size of the perimeter to a certain extent. Figure 7f shows that the lowest median line of Bainong 207 means the smallest rectangularity, which indicates that the seed fills the smallest circumscribed rectangle.

From the distributions of the characteristic parameters of the five wheat varieties, the rectangularity of Luomai 26 is the largest. The perimeter and long axis length of Jinqiang 11 is the largest, and the short axis, ellipticity, and elongation are the smallest. The area of Zhoumai 22 is the largest. The perimeter, ellipticity, and elongation of Luomai 42 are the largest, and the difference between the long and short axes length is smaller. The area, perimeter, long axis, and rectangularity of Bainong 207 are the smallest. According to the analysis results, Luomai 26, Zhoumai 22, and Luomai 42 are the largest seeds among the five varieties wheat seeds; Bainong 207 has the smallest seeds. Jinqiang 11 has the largest perimeter and long axis and the smallest short axis, ellipticity, and elongation, indicating that the seeds are elongated. The above analysis results are consistent with the actual shape of wheat.

3.3. Correlation Analysis of Seed Phenotypic Characteristics and Thousand Seed Weight

The correlations between seven parameters and the thousand seed weight of five varieties wheat seeds were analysed, and the results of the correlation analysis of Luomai 26 are shown in Figure 8.

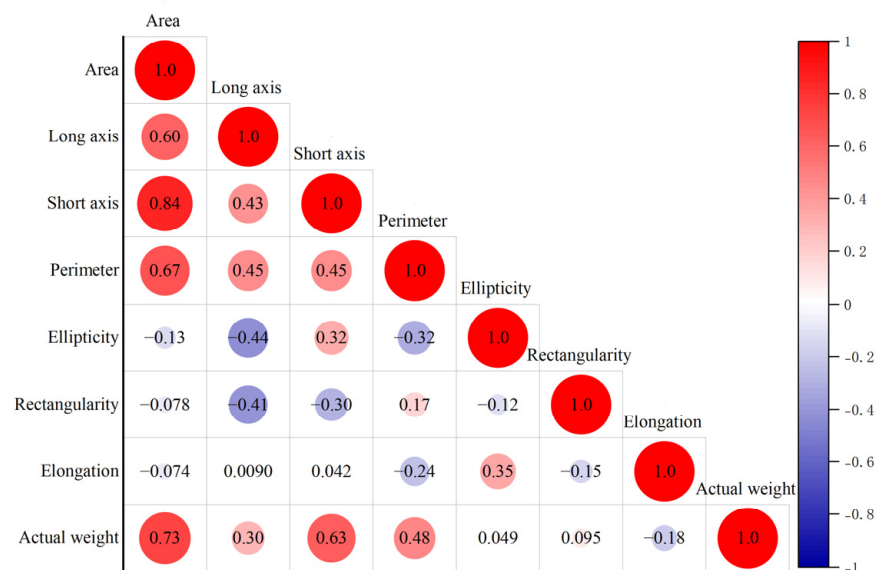


Figure 8. Matrix of the correlation coefficients between the phenotypic characteristics and thousand seed weight of Luomai 26.

As shown in Figure 8, the absolute values of the correlation coefficients of the Luomai 26 area and short axis with the thousand seed weight were 0.73 and 0.63, respectively, reaching a highly significant level ($p < 0.01$). For the other four varieties, the area, long axis, short axis, perimeter, and rectangularity of Jinqiang 11 were significantly correlated with the thousand seed weight ($p < 0.01$), with absolute values of correlation coefficients of 0.928, 0.837, 0.901, 0.850, and 0.658, respectively. The area and perimeter of Zhoumai 22 were significantly correlated with the thousand seed weight ($p < 0.01$). The absolute values of the correlation coefficients were 0.61 and 0.654, respectively. The long and short axes of Zhoumai 22 were correlated with the thousand seed weight ($p < 0.05$). The absolute values of the correlation coefficients were 0.531 and 0.481. The absolute value of the correlation coefficient between the area and thousand seed weight of Luomai 42 was 0.727, reaching a highly significant level ($p < 0.01$). The long and short axes of Luomai 42 were correlated with the thousand seed weight ($p < 0.05$). The absolute values of the correlation coefficients were 0.464 and 0.5. The area, short axis, and perimeter of Bainong 207 were significantly correlated with the thousand seed weight ($p < 0.01$), with absolute values of correlation coefficients of 0.86, 0.711, and 0.751, respectively. The absolute value of the correlation coefficient of the long axis with the thousand seed weight was 0.532, reaching a significant level ($p < 0.05$). From the above analysis, the thousand seed weight of wheat seeds was mostly related to the area, perimeter, long axis, and short axis. This result arose because the thousand seed weight of wheat seeds reflected the fullness of the seeds, which was mostly expressed in the size of the area that is to some extent related to the long axis and short axis.

3.4. Parameters and Thousand Seed Weight Model

3.4.1. Models Built

The parameters that were significantly correlated with the thousand seed weight were selected to establish a multiple linear regression model. In the process of modelling, the characteristic parameters to the 0.05 significance level were selected firstly; then, other parameters were selected in turn (according to their correlation with 1000-seed weight from high to low) to establish a multiple linear regression model, and the model with a better R^2 value was selected as the prediction model of 1000-seed weight. Table 3 shows the prediction model of superior 1000-seed weight of each wheat seed variety.

Table 3. Model for predicting thousand-grain weight of different varieties.

Varieties	Multiple Linear Regression Model	R^2	RMSE	Measured TSW (g)
Luomai 26	$y = 1.87x_1 + 1.868x_2 + 8.524$	0.497	0.668	50.800
Jinqiang 11	$y = -0.377x_1 + 10.979x_2 + 22.708x_3 - 1.948x_4 + 98.014x_6 - 137.738$	0.853	0.450	44.410
Zhoumai 22	$y = -2.021x_1 + 5.891x_2 + 14.598x_3 + 4.169x_4 - 92.814$	0.345	0.605	50.585
Luomai 42	$y = 4.717x_1 - 2.943x_2 - 8.791x_3 - 0.934x_4 + 32.189$	0.493	0.690	50.665
Bainong 207	$y = 5.068x_1 + 6.077x_2 - 22.431x_3 - 1.557x_4 + 93.483x_5 - 24.624$	0.757	0.470	44.505

Note: R^2 in the figure indicates the accuracy of the fitted model. The more R^2 tends to 1, the higher the accuracy of the model. $x_1, x_2, x_3, x_4, x_5, x_6$ and x_7 indicate the area, long axis, short axis, perimeter, ellipticity, rectangularity, and elongation parameters, respectively. Thousand seed weight (TSW).

From the five prediction models in Table 3, the thousand seed weight of Jinqiang 11 and Bainong 207 among the 20 sets of tests was approximately 44 g, and their R^2 were 0.853 and 0.757, and RMSE were 0.450 and 0.470, respectively, indicating that the accuracies of the thousand seed weight prediction models of these two varieties were higher. The thousand seed weight of Luomai 26, Zhoumai 22, and Luomai 42 were approximately 50 g, and their R^2 were below 0.5. The above analysis showed that the prediction effect of the model established in this paper was better when the thousand seed weight of wheat seeds was approximately 44 g; the prediction model was poor when the thousand seed weight

was approximately 50 g. The model in this paper had different prediction effects when it was applied to different varieties of wheat seeds.

To verify the above conclusions, wheat seeds with 40–50 g thousand seed weight were selected to analyse wheat seeds for which the model of this paper was applicable. Therefore, three wheat seeds with different fullness levels, Meichun 101, Luohan 7 and Luomai 38, in which their average thousand seed weight were 42.815 g, 47.470 g, and 49.385 g, respectively, were selected to build a thousand seed weight prediction model using the method described in this paper; their thousand seed weight was measured as shown in Table 4.

Table 4. Multiple linear regression models for the thousand seed weight of wheat seeds of three different varieties.

Varieties	Multiple Linear Regression Model	R^2	RMSE	Measured TSW (g)
Meichun 101	$y = 8.396x_1 - 6.035x_2 - 15.226x_3 - 5.445x_4 + 101.058$	0.575	0.605	42.815
Luohan 7	$y = 4.723x_1 - 5.1844x_2 + 13.289x_3 - 4.467x_4 - 12.668x_5 + 47.553$	0.815	0.599	47.470
Luomai 38	$y = 3.555x_1 + 0.063x_2 + 1.961x_3 - 1.854x_4 + 13.605$	0.569	0.723	49.385

From Table 4, the R^2 and RMSE of the prediction model of Meichun 101 were 0.575 and 0.605, respectively, and the thousand seed weight was 42.815 g. The R^2 and RMSE of the prediction model of Luohan 7 were 0.815 and 0.599, respectively, and the thousand seed weight was 47.470 g. The R^2 and RMSE of the prediction model of Luomai 38 were 0.569 and 0.723, respectively, and the thousand seed weight was 49.385 g. It can be seen from this, when the thousand seed weight of wheat seeds ranged from 40 g to 47 g, the accuracies of the prediction models built by extracting the seven characteristics were compared with those of Jinqiang 11, which had a higher R^2 of 0.853, and Zhoumai 22, which had a lower accuracy with an R^2 of 0.345.

3.4.2. Model Comparison Analysis

Jinqiang 11, Bainong 207, and Luohan 7, three varieties of wheat seeds with high accuracies in Section 3.4.1, were selected. First, principal components were selected as input variables based on the principle of a cumulative contribution rate greater than 95%; the thousand seed weight prediction model was established based on principal component analysis–multiple linear regression (PCA–MLR) [32]. Furthermore, K-fold cross-validation was applied. The models of Jinqiang 11, Bainong 207, and Luohan 7 are shown as a1, b1, and c1 in Figure 9, respectively. Meanwhile, the multiple linear regression model was established by using the characteristic parameters that are significantly related to 1000-seed weight in Section 3.4.1 [33], and the K-fold cross-validation model was adopted. The models of Jinqiang 11, Bainong 207, and Luohan 7 are shown in Figure 9(a2,b2,c2), respectively.

By comparing the different thousand seed weight prediction models established by the two methods for the same species, the accuracy of the thousand seed weight prediction models established using multiple linear regression improved by 0.01, 0.09, and 0.12 for Jinqiang 11, Bainong 207, and Luohan 7, respectively, indicating that the accuracies of the models established by multiple linear regression were better.

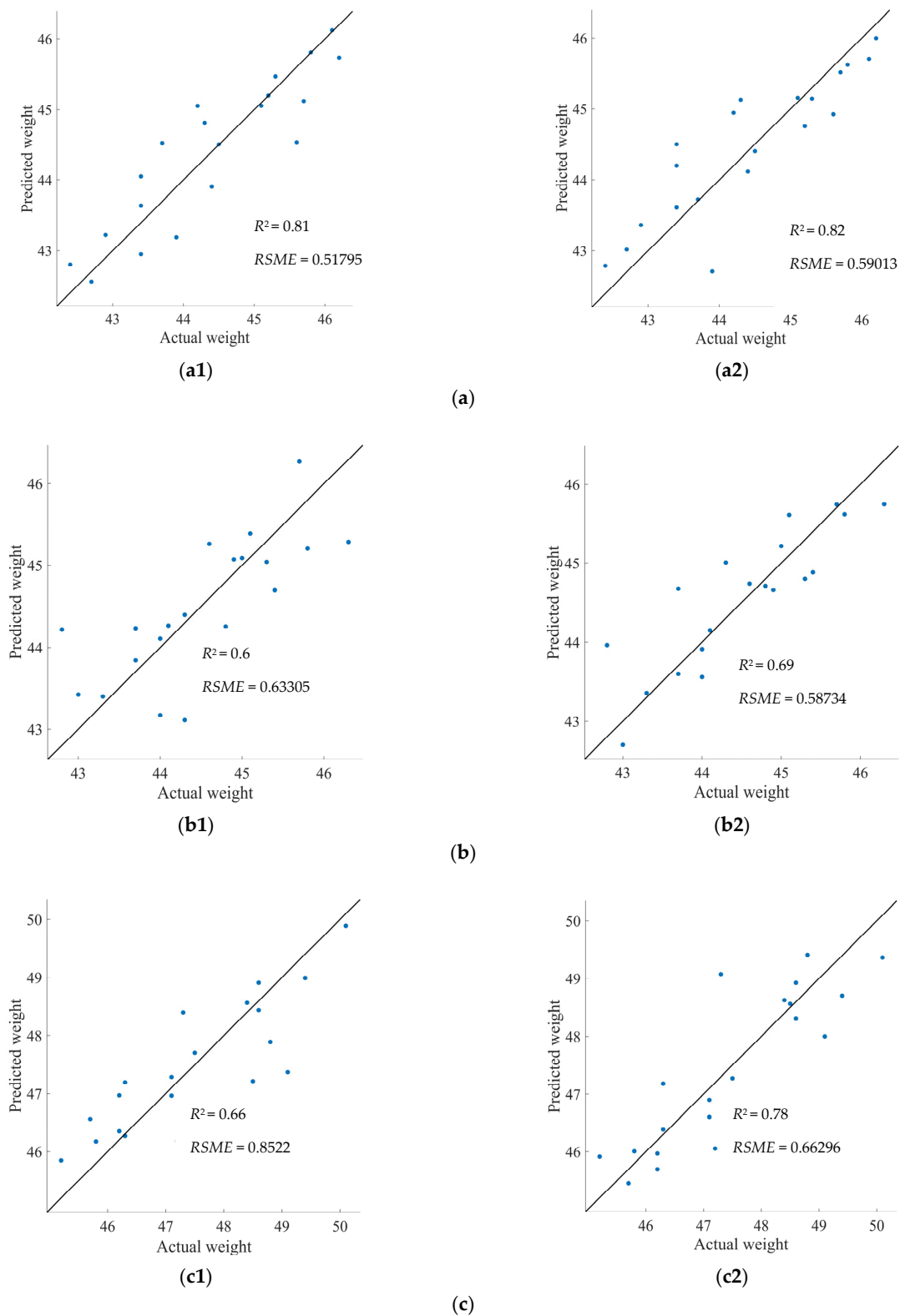


Figure 9. Predictive model validation. (a1) Predictive model based on PCA-MLR. (a2) Multiple linear regression prediction model. (a) Thousand seed weight prediction model of Jinqiang 11. (b1) Predictive model based on PCA-MLR. (b2) Multiple linear regression prediction model. (b) Thousand seed weight prediction model of Bainong 207. (c1) Predictive model based on PCA-MLR. (c2) Multiple linear regression prediction model. (c) Thousand seed weight prediction model of Luohan 7.

3.5. Discussion

The above analysis revealed that the area and short axis of Luomai 26 were significantly correlated with the thousand seed weight. The area, long axis, short axis, perimeter, and rectangularity of Jinqiang 11 were all significantly correlated with the thousand seed weight. The area and perimeter of Zhoumai 22 were significantly correlated with the thousand seed weight, and the long and short axes were correlated with the thousand seed weight. The area of Luomai 42 were significantly correlated with the thousand seed weight, and the long and short axes were correlated with the thousand seed weight. The area, short axis, and perimeter of Bainong 207 were significantly correlated with the thousand seed weight, and the long axis was correlated with the thousand seed weight. The thousand seed weight of wheat seeds was mostly correlated with the area, perimeter, long axis, and short axis, which was consistent with the results of Cui [34], who studied whether the length and width of wheat seeds significantly correlated with the thousand seed weight. The reason for this phenomenon was that the areas of wheat seeds reflected their fullness characteristics to some extent; if wheat seeds were ellipsoid, the long and short axes of wheat seeds were correlated with the perimeter and area.

A multiple linear regression model for thousand seed weight was established using significantly correlated characteristic parameters. The analysis revealed that the thousand seed weight of Jinqiang 11 and Bainong 207 was approximately 44 g among the 20 sets of tests measured; their R^2 values were 0.853 and 0.757, respectively, indicating that the prediction accuracies of the thousand seed weight prediction models for these two varieties were higher. The thousand seed weight of Luomai 26, Zhoumai 22, and Luomai 42 were approximately 50 g, and their R^2 values were below 0.5. Hence, wheat seeds with 40–50 g thousand seed weight were selected for modelling analysis. The R^2 of the prediction model of Meichun 101 was 0.575 and the thousand seed weight was 42.815 g. The R^2 of the prediction model of Luohan 7 was 0.815 and the thousand seed weight was 47.470 g. The R^2 of the prediction model of Luomai 38 was 0.569 and the thousand seed weight was 49.385 g. According to comparative analysis, the thousand seed weight prediction model established in this paper had a better prediction accuracy when the thousand seed weight was 44–47 g and could better reflect the fullness ranges of wheat seeds.

However, the more significantly correlated the characteristic parameters of wheat seeds were, the higher the accuracy of the established multiple linear regression model. For example, Jinqiang 11 had five phenotypic characteristic parameters that were significantly correlated with the thousand seed weight, and the R^2 of the established model was 0.853. The area, short axis, and perimeter of Bainong 207 were significantly correlated with the thousand seed weight, the long axis was correlated with the thousand seed weight, and the R^2 of the established model was 0.757. For Luomai 26, the area and short axis were significantly correlated with the thousand seed weight. Zhoumai 22 had two characteristic parameters (area and perimeter) that were significantly correlated with the thousand seed weight, and two parameters (long axis and short axis) were correlated with the thousand seed weight. The area of Luomai 42 was significantly correlated with the thousand seed weight, and the long and short axes were correlated with the thousand seed weight. Thus, it can be seen that the more significantly correlated the phenotypic characteristic parameters were, the higher the accuracy of the established thousand seed weight prediction model.

The correlation coefficients of each characteristic parameter with the thousand seed weight were further analysed for Luomai 26, Zhoumai 22, and Luomai 42. The correlation coefficients of the area and short axis with the thousand seed weight for Luomai 26 were 0.73 and 0.63, respectively, which were highly significant, and the R^2 of the established model was 0.497. The correlation coefficients of area and perimeter with the thousand seed weight for Zhoumai 22 were 0.61 and 0.654, the correlation coefficients of long and short axes with the thousand seed weight were 0.531 and 0.481, respectively, and the R^2 of the established model was 0.345. The correlation coefficients of the area and thousand seed weight of Luomai 42 were 0.727, the correlation coefficients of the long and short axes with the thousand seed weight were 0.464 and 0.5, and the R^2 of the established model was 0.493.

Thus, it can be seen that the higher the correlation coefficient of the significantly correlated characteristic parameters were, the higher the accuracy of the prediction model based on these characteristic parameters.

In summary, the thousand seed weights of wheat seeds were mostly related to the area, perimeter, long axis, and short axis, and different varieties of wheat seeds had different phenotypic characteristic parameters related to the thousand seed weight. When the thousand seed weight was 44–47 g, the thousand seed weight prediction model established in this paper had good accuracy and better reflected the fullness ranges of wheat seeds. The more significantly correlated the phenotypic parameters were, the higher the accuracy of the prediction model built for the thousand seed weight. The higher the correlation coefficient of significantly correlated characteristic parameters were, the higher the precision of the prediction model based on these characteristic parameters.

Although the R^2 of the prediction model established for Jinqiang 11 reached 0.853, it essentially met the demand of thousand seed weight prediction. However, there was still some error, which could be affected by the hole of the plate or the light source. Thus, the next step was to try to improve the accuracy of the prediction model by adjusting the hole of the plate or light source. In addition, due to the few varieties of wheat seeds analysed in this paper, if it was confirmed that the thousand seed weights of wheat seeds were 44–47 g, to establish whether the thousand seed weight prediction model established in this paper had a better application effect, more varieties of wheat seeds in this interval must be analysed. Furthermore, the prediction model of different crops, such as corn seeds and rice seeds, could be studied to improve the universality of the detection device.

4. Conclusions

1. A wheat seed phenotypic characteristic parameter detection system was established to extract the phenotypic characteristic parameters of five wheat seeds: Luomai 26, Zhoumai 22, Luomai 42, Jinqiang 11, and Bainong 207. The distributions of phenotypic characteristic parameters showed that Luomai 26, Zhoumai 22, and Luomai 42 were the larger seeds among the five varieties, and Bainong 207 was the smaller seed. Jinqiang 11 had the largest perimeter and long axis, and the smallest short axis, ellipticity, and elongation; thus, the seeds were elongated. Luomai 42 had the largest roundness with a small difference between the long and short axes.
2. The correlations between the phenotypic characteristic parameters of wheat seeds and thousand seed weight were analysed. The results showed that most of thousand seed weight of wheat seeds were correlated with the area, perimeter, long axis, and short axis. The phenotypic characteristics with significant correlations were different for various varieties of wheat seeds. Among them, the correlations between area, short axis, and thousand seed weight of Luomai 26 reached highly significant levels ($p < 0.01$) with coefficients of 0.73 and 0.63; the area, long axis, short axis, perimeter, and rectangularity of Jinqiang 11 all had highly significant correlations ($p < 0.01$) with the thousand seed weight with coefficients of 0.928, 0.837, 0.901, 0.850, and 0.658, respectively. The correlation between the area, perimeter and thousand seed weight of Zhoumai 22 reached a highly significant level ($p < 0.01$) with correlation coefficients of 0.61 and 0.654; the correlation between area and thousand seed weight of Luomai 42 reached a highly significant level ($p < 0.01$) with a correlation coefficient of 0.727; the correlations between area, short axis, perimeter, and thousand seed weight of Bainong 207 reached highly significant levels ($p < 0.01$) with correlation coefficients of 0.86, 0.711, and 0.751.
3. A multiple linear regression model was developed using significantly correlated phenotypic parameters, in which the R^2 of the prediction models for Jinqiang 11 and Bainong 207 were 0.853 and 0.757, respectively; the R^2 of the prediction models for Luomai 26, Zhoumai 22, and Luomai 42 were all lower than 0.5. The models were further validated by selecting wheat seeds with thousand seed weights of 40–50 g, in which the R^2 of the prediction models for Meichun 101, Luohan 7, and Luomai 38

were 0.575, 0.815, and 0.569, respectively. The modelling and validation showed that the model established in this paper had better results in predicting the thousand seed weight of wheat seeds when the thousand seed weight was 44–47 g.

Author Contributions: H.Z.: Methodology, Software, Writing, Editing, Data analysis, Result verification; J.J.: Funding acquisition, Supervision; H.M.: Methodology, Supervision; H.G.: Visualization; N.L.: Editing, Data analysis; H.C.: Methodology, Review, Editing & Supervision. All authors have read and agreed to the published version of the manuscript.

Funding: The present research was supported by 2020 Training Plan for Young Backbone Teachers in Colleges and Universities of Henan Province (No.2020GGJS075), Henan Science and Technology Research Program (No.222102110215), Henan Science and Technology Research Program(No.222102110105) and the Major Science and Technology Project of Henan Province (No.221100110800).

Institutional Review Board Statement: Not applicable.

Informed Consent Statement: Not applicable.

Data Availability Statement: The data presented in this study are available on request.

Conflicts of Interest: The authors declare no conflict of interest.

References

1. Announcement by the National Bureau of Statistics on 2022 Summer Grain Production Data. *Grain Process.* **2022**, *47*, 95.
2. Zhou, L. Research on Phenotype Information Perception Method of Wheat Based on Spectra and Images. Bachelor's Thesis, Zhejiang University, Hangzhou, China, 2022.
3. Liang, L. Research on Wheat Grain Classification Technology Based on Improved Hierarchical Analysis. Master's Thesis, Hebei Agricultural University, Baoding, China, 2013.
4. Sun, J.; Zhang, L.; Zhou, X.; Wu, X.H.; Shen, J.F.; Dai, C.X. Detection of rice seed vigor levels using hyperspectral image depth features. *J. Agric. Eng.* **2021**, *37*, 171–178.
5. Zhao, H.M.; Ge, C.J.; Jia, J.Q.; Zhang, S.J. A high-throughput phenotyping system for wheat seeds based on image analysis. *Shandong Agric. Sci.* **2021**, *53*, 113–120.
6. Wang, J.C.; Gao, Z.F.; Li, D.S.; Zhu, D.M.; Wu, H.Y. Research on the application of agricultural information technology in wheat breeding. *J. Crop* **2018**, *184*, 37–43.
7. Taner, A.; Oztekin, Y.B.; Tekguler, A.; Sauk, H.; Duran, H. Classification of Varieties of Grain Species by Artificial Neural Networks. *Agron.-Basel* **2018**, *8*, 123. [[CrossRef](#)]
8. Chen, X.; Xun, Y.; Li, W.; Zhang, J.X. Combining discriminant analysis and neural networks for corn variety identification. *Comput. Electron. Agric.* **2010**, *71*, S48–S53. [[CrossRef](#)]
9. Pourreza, A.; Pourreza, H.; Abbaspour-Fard, M.H.; Sadrnia, H. Identification of nine Iranian wheat seed varieties by textural analysis with image processing. *Comput. Electron. Agric.* **2012**, *83*, 102–108. [[CrossRef](#)]
10. Yang, S.; Zheng, L.H.; He, P.; Wu, T.; Sun, S.; Wang, M.J. High-throughput soybean seeds phenotyping with convolutional neural networks and transfer learning. *Plant Methods* **2021**, *17*, 50. [[CrossRef](#)]
11. Colmer, J.; O'Neill, C.M.; Wells, R.; Bostrom, A.; Reynolds, D.; Websdale, D.; Shiralagi, G.; Lu, W.; Lou, Q.J.; Le Cornu, T.; et al. SeedGerm: A cost-effective phenotyping platform for automated seed imaging and machine-learning based phenotypic analysis of crop seed germination. *New Phytol.* **2020**, *228*, 778–793. [[CrossRef](#)]
12. Korohou, T.; Okinda, C.; Li, H.K.; Cao, Y.F.; Nyalala, I.; Huo, L.F.; Potcho, M.; Li, X.; Ding, Q.S. Wheat grain yield estimation based on image morphological properties and wheat biomass. *J. Sens.* **2020**, *2020*, 1571936. [[CrossRef](#)]
13. Zhang, H.; Li, H.P.; Ye, J. Research on morphological characteristics of wheat grain appearance. *Grain Feed. Ind.* **2013**, *311*, 7–9.
14. Li, Z.; Liao, T.Q.; Feng, Q.C.; Zhang, D.Y.; Wang, Q.; Wang, X.N.; Zhang, L.H.; Wang, X. Design of cucumber seed vigor index detection system based on image processing technology. *Seeds* **2015**, *34*, 111–115.
15. Majumdar, S.; Javas, D.S. Classification of cereal grains using machine vision: I. Morphology models. *Trans. ASAE* **2000**, *43*, 1669–1675. [[CrossRef](#)]
16. Wang, Z.J.; Cong, P.S.; Zhou, J.L.; Zhou, Z.L. A method for evaluating wheat grain appearance quality based on image processing and artificial neural network. *J. Agric. Eng.* **2007**, 158–161.
17. Qadri, S.; Qadri, S.F.; Razzaq, A.; Rehman, M.U.I.; Ahmad, N.; Nawaz, S.A.; Saher, N.; Akhtar, N.; Khan, D.M. Classification of canola seed varieties based on multi-feature analysis using computer vision approach. *Int. J. Food Prop.* **2021**, *24*, 493–504. [[CrossRef](#)]
18. Javanmardi, S.; Ashtiani, S.H.M.; Verbeek, F.J.; Martynenko, A. Computer-vision classification of corn seed varieties using deep convolutional neural network. *J. Stored Prod. Res.* **2021**, *92*, 101800. [[CrossRef](#)]
19. He, H.X. Research on the Classification Model of Wheat Seed Varieties Based on Machine Vision. Master's Thesis, Anhui Agricultural University, Hefei, China, 2018.

20. Kara, M.; Sayinci, B.; Elkoca, E.; Ozturk, I.; Ozmen, T.B. Seed size and shape analysis of registered common bean (*Phaseolus vulgaris* L.) cultivars in Turkey using digital photograohy. *J. Agric. Sci.* **2013**, *19*, 219–234.
21. Tanabata, T.; Shibaya, T.; Hori, K.; Ebana, K.; Yano, M. SmartGrain: High-throughput phenotyping software for measuring and seed shape through image analysis. *Plant Physiol.* **2012**, *160*, 1870–1880. [[CrossRef](#)]
22. Sabanci, K.; Kayabasi, A.; Toktas, A. Computer vision-based method for classification of wheat grains using artificial neural network. *J. Sci. Food Agric.* **2017**, *97*, 2588–2593. [[CrossRef](#)]
23. Xia, X. Research on Wheat Variety Identification Based on Computer Vision. Master's Thesis, Henan University of Technology, Zhengzhou, China, 2011.
24. Fan, C.; Xia, X.; Shi, X.F.; Hou, L.D. Research on wheat variety classification based on optimization neural network. *J. Henan Univ. Technol. (Nat. Sci. Ed.)* **2012**, *33*, 72–76.
25. Choudhary, R.; Paliwal, J.; Jayas, D.S. Classification of cereal grains using wavelet, morphological, colour, and textural features of non-touching kernel images. *Biosyst. Eng.* **2008**, *99*, 330–337. [[CrossRef](#)]
26. Manickavasagan, A.; Sathya, G.; Jayas, D.S. Comparison of illuminations to identify wheat classes using monochrome images. *Comput. Electron. Agric.* **2008**, *63*, 237–244. [[CrossRef](#)]
27. Pazoki, A.R.; Pazoki, Z. Classification system for rain fed wheat grain cultivars using artificial neural network. *Afr. J. Biotechnol.* **2011**, *10*, 8031–8038.
28. Ma, Y.H.; Han, Y. Color image segmentation method. *Sci. Technol. Inf. Dev. Econ.* **2006**, *16*, 158–159.
29. Cui, Y. *Image Processing and Analysis—Mathematical Morphology Methods and Applications*; Science Press: Beijing, China, 2009.
30. Gegas, V.C.; Nazari, A.; Griffiths, S.; Simmonds, J.; Fish, L.; Orford, S.; Sayers, L.; Doonan, J.H.; Snape, J.W. A genetic framework for grain size and shape variation in wheat. *Plant Cell* **2010**, *22*, 1046–1056. [[CrossRef](#)]
31. Feng, L.J.; Li, X.J.; Wen, C.L. Wheat variety identification based on sparse representation. *J. Jiangnan Univ. (Nat. Sci. Ed.)* **2015**, *14*, 730–735.
32. Abdipour, M.; Younessi-Hmazekhanlu, M.; Ramazani, S.H.R.; Omid, A.H. Artificial neural networks and multiple linear regression as potential methods for modeling seed yield of safflower (*Carthamus tinctorius* L.). *Ind. Crops Prod.* **2018**, *127*, 185–194. [[CrossRef](#)]
33. Abdipour, M.; Ebrahimi, M.; Lzadi-Darbandi, A.; Mastrangelo, A.M. Association between Grain Size and Shape and Quality Traits, and Path Analysis of Thousand Grain Weight in Iranian Bread Wheat Landraces from Different Geographic Regions. *Not. Bot. Horti Agrobot. Cluj-Napoca* **2016**, *44*, 228–236. [[CrossRef](#)]
34. Cui, F.; Ding, A.M.; Li, J.; Zhao, C.H.; Li, X.F.; Feng, D.S.; Wang, X.Q.; Wang, L.; Gao, J.R.; Wang, H.G. Wheat kernel dimensions: How do they contribute to kernel weight at an individual QTL level? *J. Genet.* **2011**, *90*, 409–425. [[CrossRef](#)] [[PubMed](#)]

Disclaimer/Publisher's Note: The statements, opinions and data contained in all publications are solely those of the individual author(s) and contributor(s) and not of MDPI and/or the editor(s). MDPI and/or the editor(s) disclaim responsibility for any injury to people or property resulting from any ideas, methods, instructions or products referred to in the content.